Defence Research and Development Canada
Recherche et développement pour la défense Canada

DEFENCE R&D DÉFENSE

Calibrated infrared measurement of point targets using an extended source calibration methodology

P. Chevrette
DRDC Valcartier

Defence R&D Canada – Valcartier
Technical Memorandum
DRDC Valcartier TM 2004-076
January 2005

Canada

Report Documentation Page

Form Approved
OMB No. 0704-0188

1. REPORT DATE	2. REPORT TYPE	3. DATES COVERED
JAN 2005		**-**

4. TITLE AND SUBTITLE	5a. CONTRACT NUMBER
Calibrated infrared measurement of point targets using an extended source calibration methodology	5b. GRANT NUMBER
	5c. PROGRAM ELEMENT NUMBER
6. AUTHOR(S)	5d. PROJECT NUMBER
	5e. TASK NUMBER
	5f. WORK UNIT NUMBER
7. PERFORMING ORGANIZATION NAME(S) AND ADDRESS(ES) **Defence R&D Canada -Ottawa,3701 Carling Ave,Ottawa Ontario,CA,K1A 0Z4**	8. PERFORMING ORGANIZATION REPORT NUMBER
9. SPONSORING/MONITORING AGENCY NAME(S) AND ADDRESS(ES)	10. SPONSOR/MONITOR'S ACRONYM(S)
	11. SPONSOR/MONITOR'S REPORT NUMBER(S)

12. DISTRIBUTION/AVAILABILITY STATEMENT
Approved for public release; distribution unlimited

13. SUPPLEMENTARY NOTES
The original document contains color images.

14. ABSTRACT
see report

15. SUBJECT TERMS

16. SECURITY CLASSIFICATION OF:			17. LIMITATION OF ABSTRACT	18. NUMBER OF PAGES	19a. NAME OF RESPONSIBLE PERSON
a. REPORT	b. ABSTRACT	c. THIS PAGE			
unclassified	**unclassified**	**unclassified**		**34**	

Calibrated infrared measurement of point targets using an extended source calibration methodology

Paul Chevrette
DRDC Valcartier

Defence Research & Development Canada - Valcartier

Technical memorandum

DRDC Valcartier TM 2004-076

January 2005

Author

Paul Chevrette

Approved by

Gabriel Otis

Section Head, DASO

Approved for release by

Gilles Bérubé

Chief Scientist

Abstract

A methodology has been developed at DRDC Valcartier for the calibration of infrared (IR) cameras when taking IR signature measurements of military targets. This methodology is the basis of WinISAS (Windows Infrared Signature Analysis Software) developed at DRDC Valcartier for the radiometric analysis of IR imagery and consists of a radiometric calibration of the grey levels in the image, using extended reference blackbody sources. The methodology has been developed and used mainly for the IR signature analysis of extended targets, fully resolved by the camera IR sensor. The purpose of this memorandum is to demonstrate that the same methodology and WinISAS software can be applied to the measurement of point targets, which are targets with an angular coverage smaller than the individual detector element angular coverage in an image acquired from a two-dimensional IR focal plane array camera.

Résumé

RDDC Valcartier a mis au point une méthodologie pour l'étalonnage de caméras à infrarouge (IR) lors de la prise de mesures de la signature IR de cibles militaires. Cette méthodologie est la base du logiciel WinISAS (Windows Infrared Signature Analysis Software) développé à RDDC Valcartier pour l'analyse radiométrique d'images IR et consiste en un étalonnage radiométrique des niveaux de gris de l'image à partir de corps noirs de référence de grandes dimensions. Cette méthodologie a été mise au point principalement pour l'analyse de la signature IR de cibles étendues, complètement résolues par le capteur IR de la caméra. L'objectif de ce mémorandum est de démontrer que la même méthodologie ainsi que le logiciel WinISAS peuvent s'appliquer à la mesure de cibles ponctuelles, c'est-à-dire des cibles de couverture angulaire plus petite que celle d'un élément de la matrice, dans une image obtenue par une matrice bi-dimensionnelle de détecteurs IR au plan focal de la caméra.

This page intentionally left blank.

Executive summary

A methodology has been developed at DRDC Valcartier for the calibration of infrared (IR) cameras when taking IR signature measurements of military targets. This methodology, documented in Refs. 1 and 2, is the basis of WinISAS (Windows Infrared Signature Analysis Software), developed at DRDC Valcartier for the radiometric analysis of IR imagery. It consists of a radiometric calibration of the grey levels in the image, using extended reference blackbody sources. The methodology has been developed and used mainly for the IR signature analysis of extended targets, fully resolved by the camera IR sensor.

The Naval Engineering Test Establishment (NETE) has used WinISAS for the analysis of the IR data from many trials, and more recently, for the analysis of the co-recorded calibrated IR video data collected during the SIRIUS trials in the Bahamas onboard the HMCS Montreal, from 6 to 24 October 2003. Questions have been raised about the applicability of the DRDC Valcartier calibration and analysis methodology when using extended (well-resolved) reference sources to calibrate the IR cameras and obtain the radiant intensity contrast (ΔI_t) of a point target.

The purpose of this memorandum is to demonstrate that the same methodology and WinISAS can be applied for the IR analysis of extended as well as point targets, which are targets with an angular coverage smaller than the individual detector element angular coverage in an image acquired from a two-dimensional IR focal plane array camera.

Since no real target is ever, in practice, a point target (because it would need to be infinitesimally small), the notion of a point target is always defined relatively to the detector element's projected area at the target range and the projected area of the imager's point-spread function (PSF). The intensity of any target is defined as its radiance times its cross-section area. By using an extended-source radiance calibration method to evaluate the intensity of a *point* target, it has been shown experimentally that, for a point target, an *apparent* radiance value is effectively determined instead of the real target radiance because the latter does not completely fill the detector element. To this *apparent* radiance is associated a projected detector element area that is larger than the actual target area, and the exact radiant intensity value is obtained when the two values are multiplied. The laboratory measurements also demonstrate that the position of the target within the field of view or the focus setting of the camera have little effect on the calculated intensity values, as expected, because the broadening of the target image caused by distortions or focus settings distributes the energy over more detector elements, thus compensating a decrease in signal by a larger apparent target area.

Chevrette P. 2004. Calibrated infrared measurement of point targets using an extended source calibration methodology. DRDC Valcartier TM 2004-076. Defence R&D Canada.

Sommaire

RDDC Valcartier a mis au point une méthodologie pour l'étalonnage de caméras à infrarouge (IR) lors de la prise de mesures de la signature IR de cibles militaires. Cette méthodologie est documentée aux ref. 1 et 2 et est à la base du logiciel WinISAS (Windows Infrared Signature Analysis Software), également mis au point à RDDC Valcartier pour l'analyse radiométrique d'images IR. Elle permet l'établissement d'une correspondance radiométrique avec les niveaux de gris dans l'image, à partir de corps noirs de référence de grandes dimensions. Cette méthodologie à été mise au point principalement pour l'analyse de la signature IR de cibles étendues, complètement résolues par le capteur IR de la caméra.

Le Centre d'essais techniques (Mer) (CETM) a utilisé WinISAS pour l'analyse des données IR de plusieurs essais, et plus récemment pour l'analyse des données vidéo IR co-enregistrées lors des essais du système SIRIUS dans les Bahamas, à bord du NCSM Montréal, du 6 au 24 octobre 2003. La méthodologie d'étalonnage et d'analyse de RDDC Valcartier, basée sur l'utilisation de sources de référence étendues (résolues) pour l'étalonnage des caméras IR, a été mise en question quant à son applicabilité au calcul du contraste en intensité (ΔI_t) de cibles ponctuelles.

Ce mémorandum a pour objectif de démontrer que la même méthodologie ainsi que le logiciel WinISAS peuvent être appliqués tant à l'analyse de cibles étendues qu'à des cibles ponctuelles, c'est-à-dire des cibles dont les dimensions angulaires sont plus petites que celles de l'élément individuel d'une matrice de détecteurs IR au plan focal de la caméra.

Puisqu'en pratique, aucune cible n'est vraiment ponctuelle (il faudrait qu'elle soit infiniment petite), la notion de cible ponctuelle est toujours définie relativement à la surface projetée d'un élément de la matrice de détecteurs à la distance de la cible ou à la surface projetée de la *fonction d'étalement* de la caméra. L'intensité de n'importe quelle cible est définie comme sa radiance énergétique multipliée par sa surface. On démontre expérimentalement qu'en utilisant une méthode d'étalonnage en radiance au moyen de sources étendues dans le cas d'une cible ponctuelle, on obtient une valeur de radiance *apparente* au lieu de la radiance réelle de la cible parce que l'image de celle-ci ne remplit pas un élément de la matrice de détecteurs. À cette radiance *apparente*, on associe la surface projetée d'un élément du détecteur qui est plus grande que la dimension réelle de la cible et on obtient la valeur exacte de l'intensité radiométrique lorsque les deux valeurs sont multipliées. Des mesures en laboratoire démontrent aussi que la position de la cible dans le champ de vision de la caméra ainsi que l'ajustement de mise au foyer ont peu d'effet sur la valeur calculée de l'intensité, puisque l'élargissement de l'image de la cible causé par des distorsions ou une mauvaise mise au point distribue l'énergie sur plusieurs éléments détecteurs, compensant de ce fait la diminution du signal par une plus grande surface apparente de la cible.

Chevrette P. 2004. Calibrated infrared measurement of point targets using an extended source calibration methodology. DRDC Valcartier TM 2004-076. R et D pour la défense Canada.

Table of contents

List of figures

List of tables

Acknowledgements

The author wishes to thank Mr. Denis Dion, Dr. Luc Forand and Mrs. Françoise Reid from DRDC Valcartier, as well as Dr. Arie DeJong from TNO, Netherlands, for their useful comments and constructive discussions during the preparation of this document.

This page intentionally left blank.

1. Introduction

A methodology has been developed at DRDC Valcartier for the calibration of infrared (IR) cameras when taking IR signature measurements of military targets. This methodology is documented in Refs. 1 and 2 and is the basis of WinISAS (Windows Infrared Signature Analysis Software), developed at DRDC Valcartier for the radiometric analysis of IR imagery. It consists of a radiometric calibration of the grey levels in the image, using extended reference blackbody sources. The methodology has been developed and used mainly for the IR signature analysis of extended targets, fully resolved by the camera IR sensor.

The Naval Engineering Test Establishment (NETE) has used WinISAS for the analysis of the results of many trials, and more recently, for the analysis of the co-recorded calibrated video data collected during the SIRIUS trials in the Bahamas onboard the HMCS Montreal, from 6 to 24 October 2003. During these trials, suspended targets were towed by a helicopter, and a fighter aircraft was also used to test the SIRIUS system. The suspended targets were considered to be point targets at longer ranges, and the target fighter aircraft can also be considered to be a point target at its maximum detection range and for a good part of its trajectory. Questions have been raised about the applicability of the DRDC calibration and analysis methodology when using extended (well resolved) reference sources to calibrate the cameras and obtain the radiant intensity contrast (ΔI_t) of a point target.

The purpose of this memorandum is to demonstrate that the same methodology and WinISAS can be applied to the measurement of extended as well as point targets, which are targets with an angular coverage smaller than the individual detector element angular coverage in an image acquired from a two-dimensional IR focal plane array camera.

2. Basic relations

The reader is referred to Refs. 1 and 2 for a complete description of DRDC Valcartier extended source calibration methodology. In brief, two external blackbody reference sources of known temperatures are placed at some known distance from the cameras and images of these sources are recorded prior to or immediately after recording images of a target. The sources must be well resolved on the detector so that its solid angle, as seen by the cameras, covers several detector element solid angles, Ω_d (see Fig. 1). Whenever possible, if the reference sources are larger than the camera's lens diameter, they can also be placed directly against the lens for calibration purpose (calibration source covers all the detector elements). Furthermore, the gain and offset settings of the camera used during the calibration should also be used when recording the target, if there is no way of converting the calibration from one setting to another. The basic idea in calibration is to establish a one-to-one correspondence between the apparent radiance L (W/m^2-sr) from any part of the imaged scene and the grey (signal)

level measured by the camera, assuming that the detector responds linearly to the incident radiometric flux Φ_d (W), which in turn is proportional to the target radiance integrated over the limits of the camera's spectral response $R(\lambda)$. A target apparent radiance is the radiance measured by the camera for a target at a known range and including the effect of atmospheric attenuation. WinISAS is designed to take the amount of atmospheric attenuation into account and to correct for its effect to obtain the unattenuated radiance of the target. Of course, when an IR image analysis is performed to extract the IR signature of a target, in most cases the results are given in contrast values, i.e. the apparent or corrected radiance of the background (selected in the scene immediately surrounding the target) is evaluated and subtracted from the measured apparent or corrected radiance of each target pixel. At this point, for simplicity, the atmospheric attenuation effect is ignored when describing the basic relations between the target radiance L_t, the incident flux Φ_{to} and the irradiance E_{to} on the camera optics from the target, and the flux Φ_{td} on a detector element, when the extent of the target is much larger than Ω_d. The exact relationships are given by Eqs 2.1 and 2.2, and their geometry is illustrated in Fig. 1.

$$\Phi_{to} = L_t A_{dt}\left(\frac{A_o}{R^2}\right) = L_t\left(\frac{A_{dt}}{R^2}\right)A_o = L_t \Omega_d A_o \tag{2.1}$$

$$E_{to} = \left(\frac{\Phi_{to}}{A_o}\right) = L_t \Omega_d \tag{2.2}$$

where:

L_t is the target radiance integrated over the spectral response of the camera;

A_{dt} is the area of the *sensitive surface* of the detector element projected on the target;

A_o is the area of the camera front optics;

R is the range of the target from the camera

To obtain contrast values, we subtract the background corresponding signal to the target signal:

$$\Delta\Phi_{to} = (L_t - L_b)\Omega_d A_o = \Delta L_t \Omega_d A_o \tag{2.1b}$$

$$\Delta E_{to} = \Delta L_t \Omega_d \tag{2.2b}$$

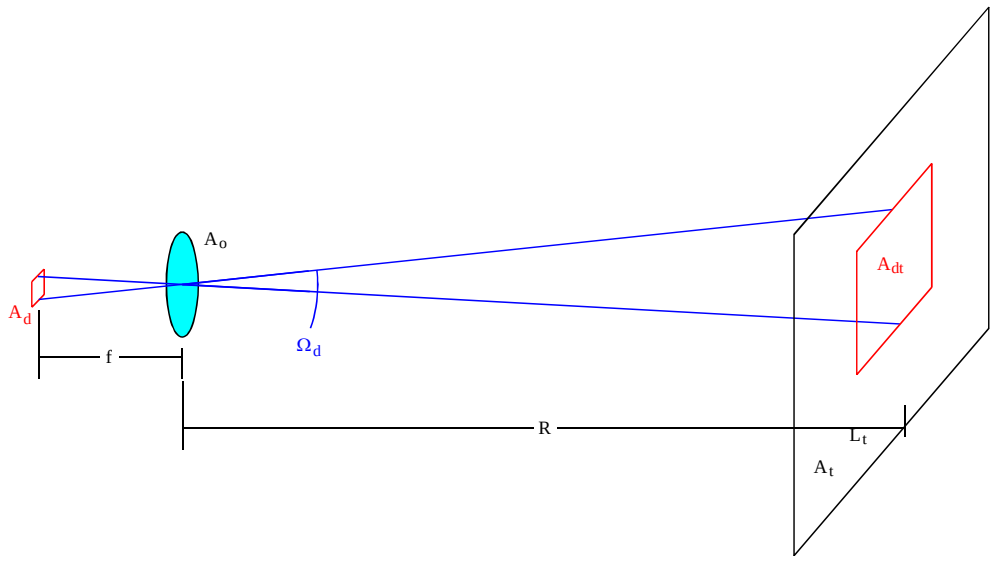

Figure 1. *Geometry describing the relationship between target and camera parameters*

Assuming no loss and no degradation of the image by the optics (geometric image), the radiometric flux contrast $\Delta\Phi_{td}$ on a detector element from the extended target is the same as $\Delta\Phi_{to}$ on the front optics, originating from the detector element's projected area in the target plane. It is obtained from the following relation:

$$\Delta\Phi_{td} = \Delta L_t \Omega_d A_o = \frac{\Delta L_t A_d A_o}{f^2} = \frac{\pi}{4}\left(\frac{\Delta L_t A_d D^2}{f^2}\right) = \frac{\pi}{4}\left(\frac{\Delta L_t A_d}{F_\#^2}\right) \qquad (2.3)$$

where:

A_d is the detector's *sensitive area* in the focal plane of the optics;

f is the focal length of the optics;

D is the diameter of the optics;

$F_\#$ is the optics f-number (f/D) of the optics.

From Eq. 2.3 it is obvious that Φ_d is directly proportional to the target radiance L_t, as the other parameters are camera specific constants.

3. Extended target and effect of the PSF

For an exact analysis of the radiometric flux hitting a detector element, the effect of image degradation caused by the optical point-spread function (*PSF*) must be taken into account. In any imaging system, the observed image results from the convolution of the perfect geometric image of the scene with the *PSF* of the front optics, also known as the blur spot. This is the best focal point that can be obtained when the effects of diffraction and optical aberration are considered. For simplicity, during the

following discussions, we will assume that the transmission factor of the front optics is 100%.

The following equation expresses the flux contrast received by a detector element from an extended target when the effect of the *PSF* is introduced into equation 2.3:

$$\Delta\Phi_{td} = \frac{\pi}{4F_{\#}^2}\int\left[PSF(x,y) * \Delta L_{ti}(x,y)\right] rect\left(\frac{x}{X_d}\right) rect\left(\frac{y}{Y_d}\right) dxdy \qquad (3.1)$$

where:

ΔLti(x,y) is the image mapping of the target radiance contrast in the focal plane;

Xd, Yd are the respective horizontal and vertical dimensions of the detector element's sensitive area;

$$rect\left(\frac{x}{X}\right) = 1 \quad \text{for} \quad -\frac{X}{2} \le x \le \frac{X}{2}\text{, 0 otherwise}$$

and the convolution (* operator) of the target radiance image with the *PSF* is given by:

$$PSF(x,y) * \Delta L_{ti}(x,y) = \int PSF(\xi - x, \eta - y) \times \Delta L_{ti}(\xi,\eta) d\xi d\eta \qquad (3.2)$$

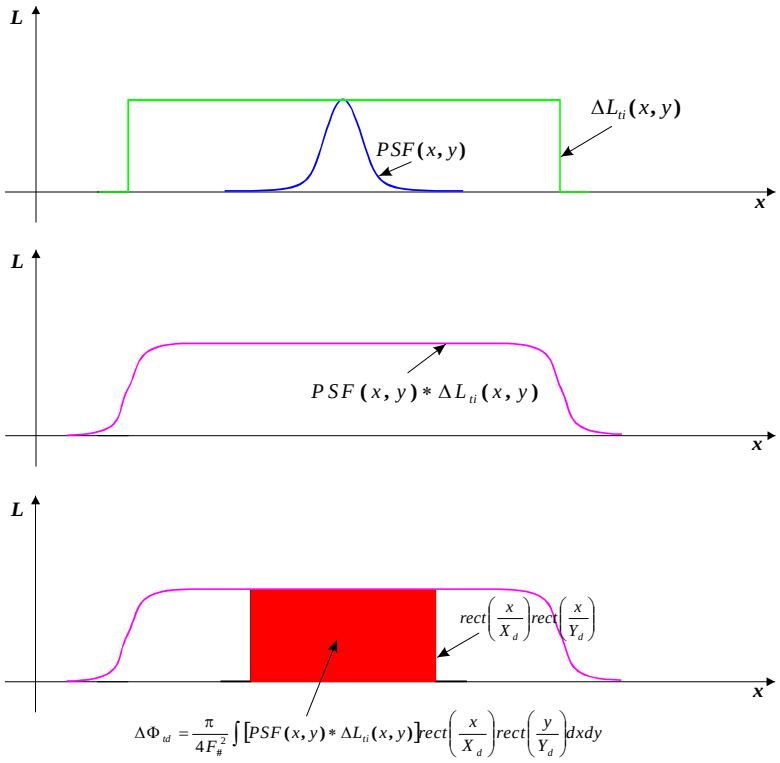

Figure 2. *Representation of steps in equation 3.1*

Equation 3.2 shows that the convolution is performed over the entire target image $L_{ti}(x,y)$ (calibrated in target radiance value). However, when the target is larger than the detector area, then the integration of the convolution function in Eq. 3.1 is limited to the detector's dimension by the *rect( )* functions. Thus, Eq. 3.1 represents the total flux received by a detector element from a uniform target that is larger in size than the solid angle seen by the detector element. This value corresponds to the area under the portion of the convolution curve delimited by the detector's *sensitive area*, as shown in Figure 2.

4. Point target and the effect of the PSF

The same equation, Eq. 3.1, applies to the description of the total flux contrast $\Delta\Phi_{td}$ resulting from a point target on a detector element. However, in this case the target image radiance contrast function $\Delta L_{ti}(x,y)$ is significantly smaller than the detector size, as shown in Figure 3. Then the convolution of the target image $\Delta L_{ti}(x,y)$ with the $PSF(x,y)$ yields a function that is very similar to the $PSF(x,y)$ function, except for a slightly larger width.

Thus, the total flux contrast $\Delta\Phi_{td}$ on a detector element is the integrated volume under the convolution surface (when considering the two dimensions). As the spatial extent of the convolution is smaller than the detector's area (when the image of the target is centered on a detector element), the measured flux is not affected by the size of the detector element, as opposed to the case of an extended target. Consequently, when the detector has been calibrated using an extended reference source of constant radiance, the measured flux contrast from a point target that falls entirely within one detector element can be interpreted as that coming from an extended target of constant apparent radiance contrast (ΔL_{t_app}) that is proportional to the measured flux contrast, $\Delta\Phi_{td}$, divided by the detector's sensitive area, similarly to Eq. 2.3. In this case, the apparent radiance contrast is given by

$$\Delta L_{t\_app} = \left(\frac{4F_{\#}^2}{\pi}\right)\left(\frac{\Delta\Phi_{td}}{A_d}\right) \tag{4.1}$$

and will always be less than the true radiance contrast, ΔL_t, of the target.We will see in the next chapter that this lower apparent radiance value, multiplied by a larger projected area than the actual target size, can give the real target radiant intensity contrast value ΔI_t (W/sr).

$$\Delta I_t = \Delta L_{t\_app} A_{dt} \tag{4.2}$$

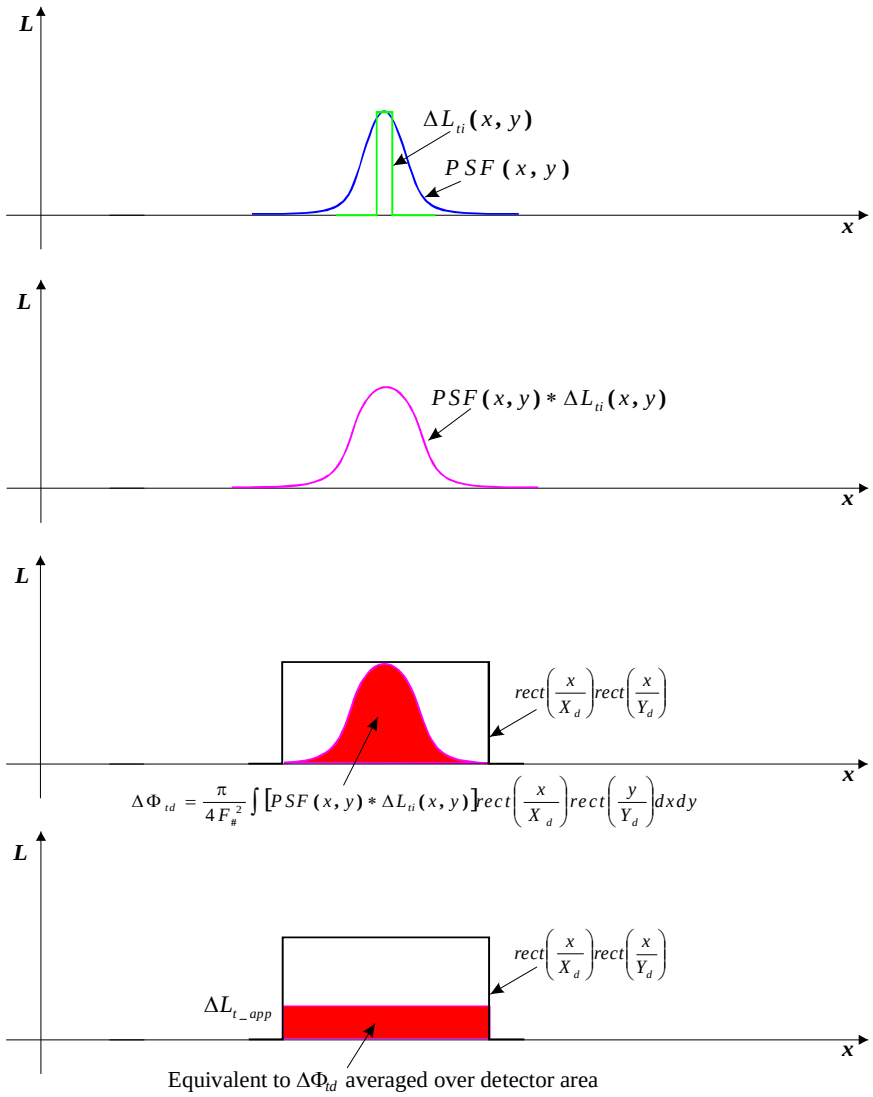

Figure 3. *Representation of steps in equation 3.1 for a point target*

5. Calibration with an extended reference source and intensity measurements

5.1 Case of large target

Assuming that the measured signal from each detector element (grey level, g) is proportional to the flux contrast, $\Delta\Phi_{td}$, incident on the detector's sensitive area, and that the calibration has been performed using an extended source, then the measured flux can be directly related to the known radiance of the reference source within the spectral response of the camera (Refs. 1 and 2).

At this point, if the camera has a 2D focal plane detector array, the notion of *fill factor* must be introduced. In most detector arrays, the detector's *sensitive area* does not cover all the space between adjacent detector elements because a part of that space is used for the layout of electrodes or wires to connect the photosensitive part to the electronic readout circuits, thus creating some dead space around the sensitive area of each detector element. The ratio between the *actual sensitive area* of the detector array and the *total area* of the detector array is called the *fill factor* (also the ratio of the sensitive area of a detector element to the total space available for each element).

When the camera outputs a direct digital image from a 2D focal-plane array, the following procedure can be used to obtain the overall intensity contrast, ΔI_t, of a uniform target whose extent is much larger than the solid angle coved by a single detector element.

Using the radiance calibration of the camera by means of an extended source, the overall target intensity is calculated from the summation of the corresponding radiance values for all the detector elements on target, multiplied by their *projected area in the target plane with a fill factor of one* (A_{dtf}). This is better accomplished by summing the histogram of the detector elements on target as a function of their grey levels, $H_t(g)$, multiplied by the corresponding radiance, $L(g)$ and detector projected area A_{dtf} (Eq. 5.1). The use of a fill factor of one when projecting the detector area onto the target plane is based on the premise that the target radiance value is the same in the dead space between the detector elements as it is on the detector element sensitive area. The overall target radiant intensity I_t (W/sr) is then obtained from

$$I_t = \sum_g L(g) H_t(g) A_{dtf} \tag{5.1}$$

where:

$L(g)$ is the calibrated radiance corresponding to grey level g;

$H_t(g)$ is the histogram of the detector elements on target as a function of grey level (number of detector elements with grey level g);

A_{dtf} is the projected area of the detector element in the target plane, with a fill factor of 1.

The target radiant intensity contrast is obtained by subtracting an equivalent area at the background radiance value:

$$\begin{aligned} \Delta I_t &= \sum_g L(g) H_t(g) A_{dtf} - \sum_g L_b H_t(g) A_{dtf} = \sum_g (L(g) - L_b) H_t(g) A_{dtf} \\ \Delta I_t &= \sum_g \Delta L(g) H_t(g) A_{dtf} \end{aligned} \tag{5.2}$$

5.2 Case of point target and PSF smaller than detector sensitive area

A target is considered as a point target when its extension is smaller than the projected *PSF* of the optical system and, in most cases also smaller than the detector element's projected *sensitive area*. In that case, Eq. 5.1 becomes:

$$I_t = L_{t\_app} A_{dt} \tag{5.3}$$

where:

L_{t_app} is the apparent radiance measured by the detector element, based on its calibration with an extended source;

A_{dt} is the *projected area* of the *sensitive* part of the detector element in the target plane.

The contrast radiant intensity is obtained similarly to Eq. 5.2:

$$\Delta I_t = (L_{t\_app} - L_b) A_{dt} = \Delta L_{t\_app} A_{dt} \tag{5.4}$$

Since, upon calibration with an extended reference source, the flux was integrated over the detector's *sensitive area*, and since the point target is smaller than that area, it is normal that, to recover the radiant intensity I_t of the target, the *projected sensitive area* of the detector element is used. Thus, the apparent radiance value L_{t_app} is lower than the target's real radiance value and is compensated by multiplying with a projected area larger than the actual target area to obtain an exact target radiant intensity value.

Note: This case is almost hypothetical because an optical designer will normally correct his design until the *PSF* approximately matches the dimensions of the detector element. Bettering the optics beyond this limit only increases costs without any additional benefits. Moreover, beyond some relatively short ranges, the turbulence effects of the atmosphere will broaden the point target image to dimensions exceeding the span of a single detector element.

5.3 Case of point target and PSF larger than detector sensitive area

In the case when the *PSF* of the optics, or the *PSF* of the optics combined with the atmospheric turbulence dispersion effect, is larger than one detector element, then Eq. 5.1 also applies to point targets since the *PSF* then overflows on neighboring detector elements. Consequently, the summation is performed over all the detector elements included in the area covered by the *PSF* convolved with the point target (atmospheric turbulence effect included), and A_{dtf} is used (detector area with a fill factor of 1.0) to compensate for the loss of energy falling on the dead space between detector elements.

However, in such a case, an effective fill factor smaller than one may have an impact on the accuracy of the measured intensity value if only a few pixels are included in the PSF. Figure 4 illustrates this effect.

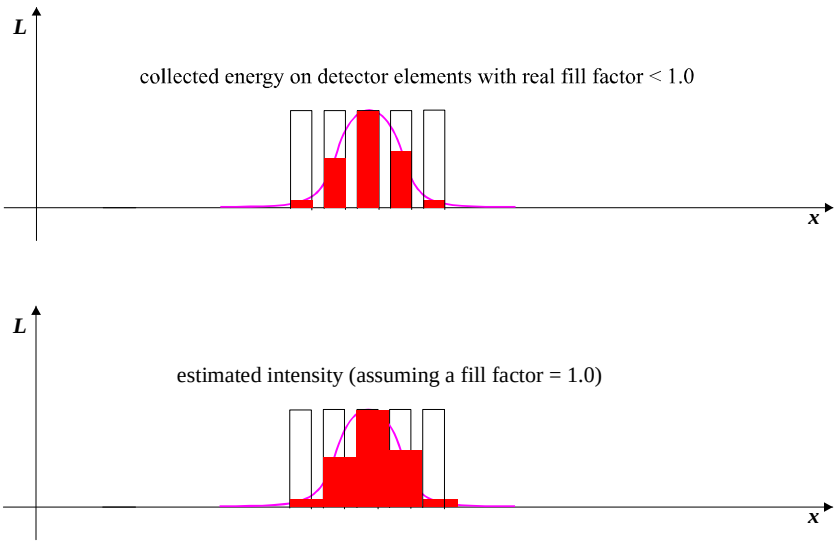

Figure 4. *Effect of an effective fill factor smaller than one on the estimated intensity*

As can be seen, the detector elements are collecting radiant energy only over their active area. if the fill factor is smaller than one and the detector element integrating on the edge of the PSF, where there is a strong gradient, the measured radiance corresponds to the average radiance over the actual detector collecting area. When this apparent radiance is converted to a radiant intensity value, the average radiance is multiplied by the projected detector area assuming a fill factor of one, therefore the same measured apparent radiance is given to the gap adjacent to the detector element. Depending of the position of the detector element with respect to the gradient signal, this leads to either an overestimate or an underestimate of the true intensity value. the smaller the number of pixel elements encompassed in the PSF, the larger the error. The error will also vary with shifting positions of the target over the detector matrix. As the number of included elements increases (more samples), this edge effect tends to becomes negligible.

5.4 Case of digitized analog image

Oftentimes, the digital signal is converted to an NTSC (or PAL) analog video output that is recorded onto analog tape before being converted back to digital format using a frame-grabber card for further analysis. In this case, no spatial relationship exists between the digital pixels and the actual detector elements in the focal-plane array. Consequently, calibration with an extended reference source should be performed following the digitization of the images with the frame-grabber such that the electronic bandpass of the analog video amplifier, the recorder and the frame-grabber are included. The above equations may then be applied using the projected area of the pixels defined by the frame-grabber instead of the projected area of the detector elements. Most likely, the additional electronic bandpass will have smoothed the discrete signal of the detector elements to a continuous signal during the digital to analog conversion so that, in this case, the fill factor is 100% and makes the individual elements indistinguishable. However, caution should always be exercised to make sure

that this is actually the case. If not, for point targets, an effective fill factor should be determined from the analog and digital signals.

6. Experimental results

To verify the above described principles, and the applicability of the calibration methodology and WinISAS to point target measurements, experimental measurements were taken in the laboratory with known blackbody references and point targets. Figure 5 illustrates the experimental set-up.

Figure 5. *Experimental setup for calibration and point target measurements*

The experimental measurements were performed with an LWIR Phoenix camera from Indigo, a focal plane array of quantum well detectors, 640 x 512 elements, operating in the 8.0 - 9.2 waveband, with a 14-bit digital output, using an 100-mm objective lens which gave a horizontal field of view of 9.2 degrees. Two extended reference blackbodies at known temperatures were used for the radiometric calibration of the camera. The target was a velvet black painted plate in which discs with pin holes of various size could be inserted, in front of a controlled blackbody whose temperature could be adjusted to obtain a reasonable signal to noise ratio. The dimensions of the plate holding the target discs could also be used for the spatial calibration, that is to obtain the pixel angular coverage and projected area, knowing the distance of the plate (3.0 meters) to the camera. One of the reference blackbodies was kept at ambient temperature (25°C), while the other was set at 90°C for an optimum coverage of the camera dynamic range. Following the grabbing of calibration images (reference blackbodies and plate of known dimensions), target images were grabbed for pinholes of different sizes, from fully resolved to sub-pixel coverage. For the sub-pixel targets, images were grabbed with the target appearing at different positions in the field of view, and with different focus settings, in order to see the effect of lens distortions and focus adjustment.

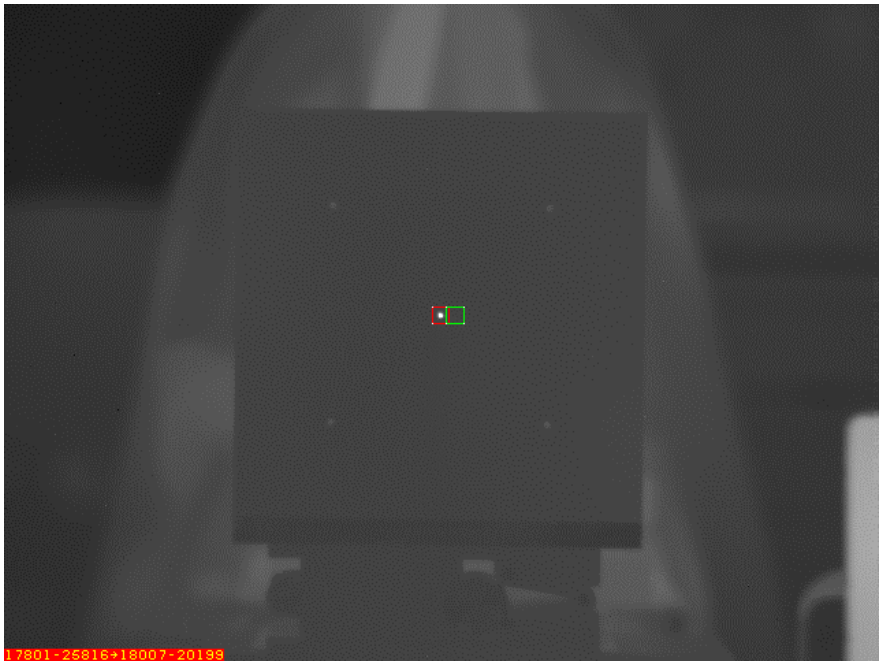

Figure 6 *Point target, 0.17 mrad diameter, centered and in-focus*

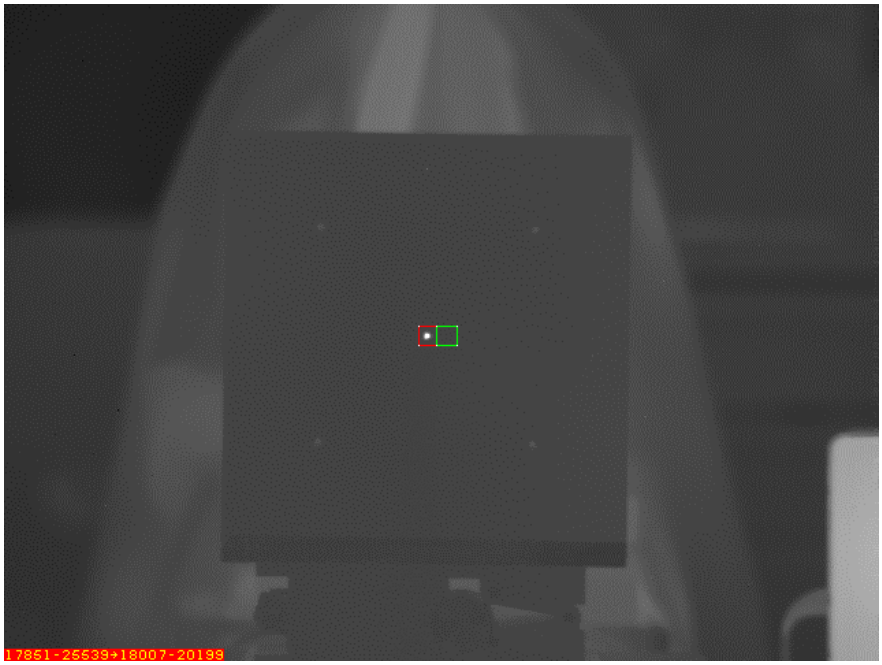

Figure 7 *Point target, 0.17 mrad diameter, centered and slightly out of focus*

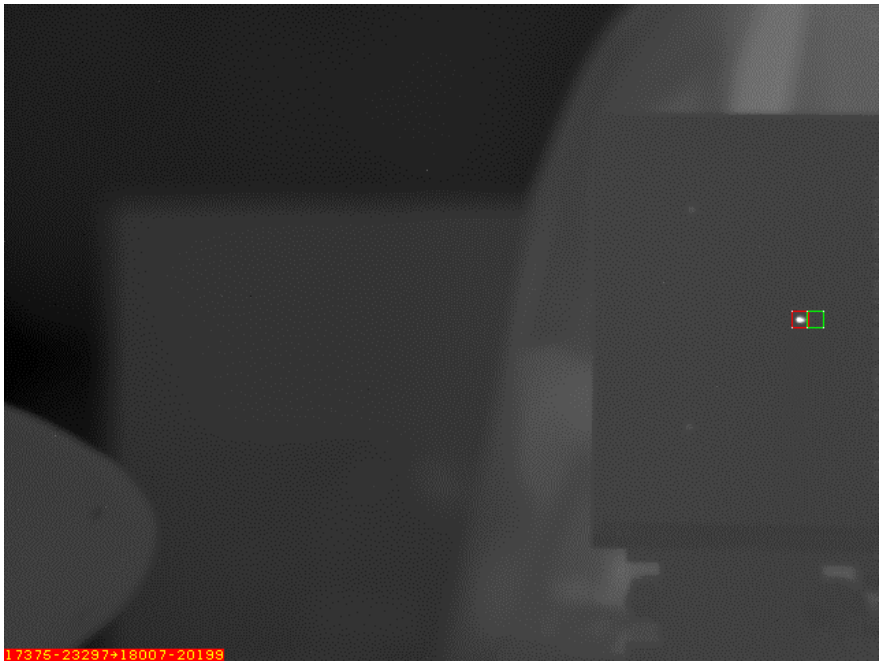

Figure 8 *Point target, 0.17 mrad diameter, to the right and with coma distortion*

Figure 9 *Point target, 0.17 mrad diameter, top and slightly out of focus*

Table 1 *Real and measured and contrast intensities for resolved and unresolved targets, using WinISAS*

Test	Tgt diam (mm)	Tgt IFOV (mr)	Tgt Temp (deg C)	Tgt L (W/sr.m2)	Bkgnd L (W/sr.m2)	Tgt area (real) (m2)	Tgt area (meas) (m2)	Tgt ΔL (meas) (W/sr.m2)	Δg	**Tgt ΔI (meas) (W/sr)**	**Tgt ΔI (real) (W/sr)**	Δ (%)	Contour type	Comments
Tests 6 et 7: BB éloigné de cible pour éliminer le réchauffement de la plaque														
6	**7.6200**	**2.5862**	90	26.96	8.9663	**4.560E-05**	2.123E-04	3.869	1524	**8.214E-04**	**8.206E-04**	0.10%	NATO	**center**
6	**5.0800**	**1.7241**	90	26.96	8.8613	**2.027E-05**	1.754E-04	2.1293	839	**3.735E-04**	**3.668E-04**	1.81%	NATO	**center**
6	**2.5400**	**0.8621**	90	26.96	8.9382	**5.067E-06**	1.255E-04	0.7519	296	**9.436E-05**	**9.132E-05**	3.34%	NATO	**center**
6	**1.2700**	**0.4310**	90	26.96	9.0149	**1.267E-06**	6.091E-05	0.3784	149	**2.305E-05**	**2.273E-05**	1.39%	NATO	**center, weak signal**
6	**0.7620**	**0.2586**	200	83.64	8.9213	**4.560E-07**	7.223E-05	0.4161	163	**3.005E-05**	**3.407E-05**	-11.79%	NATO	**center, weak signal**
6	**0.7620**	**0.2586**	200	83.64	8.9285	**4.560E-07**	7.223E-05	0.4412	173	**3.187E-05**	**3.407E-05**	-6.46%	NATO	**center, weak signal, out c**
6, 1	**0.5080**	**0.1724**	425	293.27	9.0974	**2.027E-07**	5.565E-05	0.885	337	**4.925E-05**	**5.760E-05**	-14.49%	NATO	**center, on pixel**
6, 2	**0.5080**	**0.1724**	425	293.27	9.0985	**2.027E-07**	6.623E-05	0.8743	332	**5.790E-05**	**5.760E-05**	0.54%	NATO	**center right**
6, 3	**0.5080**	**0.1724**	425	293.27	9.0737	**2.027E-07**	6.071E-05	1.0197	387	**6.191E-05**	**5.760E-05**	7.47%	NATO	**right**
6, 4	**0.5080**	**0.1724**	425	293.27	9.0750	**2.027E-07**	5.059E-05	1.0342	392	**5.232E-05**	**5.760E-05**	-9.17%	NATO	**center**
6, 5	**0.5080**	**0.1724**	425	293.27	9.1225	**2.027E-07**	7.772E-05	0.7625	289	**5.926E-05**	**5.759E-05**	2.90%	NATO	**center left**
6, 6	**0.5080**	**0.1724**	425	293.27	9.1110	**2.027E-07**	9.658E-05	0.6513	247	**6.290E-05**	**5.759E-05**	9.22%	NATO	**left**
6, 7	**0.5080**	**0.1724**	425	293.27	9.1239	**2.027E-07**	6.071E-05	0.9581	363	**5.817E-05**	**5.759E-05**	1.00%	NATO	**top**
6, 8	**0.5080**	**0.1724**	425	293.27	9.0718	**2.027E-07**	7.772E-05	0.7833	363	**6.088E-05**	**5.760E-05**	5.69%	NATO	**bottom**
6, 9	**0.5080**	**0.1724**	425	293.27	9.1117	**2.027E-07**	7.772E-05	0.6286	396	**4.885E-05**	**5.759E-05**	-15.17%	NATO	**center, on pixel**
6, 1	**0.5080**	**0.1724**	425	293.27	9.1047	**2.027E-07**	7.175E-05	0.7749	293	**5.560E-05**	**5.760E-05**	-3.47%	NATO	**center, out of focus**
6, 2	**0.5080**	**0.1724**	425	293.27	9.1012	**2.027E-07**	8.370E-05	0.6632	252	**5.551E-05**	**5.760E-05**	-3.62%	NATO	**center right, out of focus**
6, 3	**0.5080**	**0.1724**	425	293.27	9.0646	**2.027E-07**	6.477E-05	0.8945	339	**5.794E-05**	**5.760E-05**	0.58%	NATO	**right, out of focus**
6, 4	**0.5080**	**0.1724**	425	293.27	9.1023	**2.027E-07**	7.772E-05	0.7265	276	**5.646E-05**	**5.760E-05**	-1.97%	NATO	**center left, out of focus**
6, 5	**0.5080**	**0.1724**	425	293.27	9.1189	**2.027E-07**	8.278E-05	0.6867	260	**5.685E-05**	**5.759E-05**	-1.30%	NATO	**left, out of focus**
6, 6	**0.5080**	**0.1724**	425	293.27	9.1136	**2.027E-07**	8.370E-05	0.7006	266	**5.864E-05**	**5.759E-05**	1.82%	NATO	**center top, out of focus**
6, 7	**0.5080**	**0.1724**	425	293.27	9.1156	**2.027E-07**	7.772E-05	0.7554	287	**5.871E-05**	**5.759E-05**	1.94%	NATO	**top, out of focus**
6, 8	**0.5080**	**0.1724**	425	293.27	9.0868	**2.027E-07**	6.071E-05	0.8787	333	**5.335E-05**	**5.760E-05**	-7.38%	NATO	**center bottom, out of focu**
6, 9	**0.5080**	**0.1724**	425	293.27	9.0758	**2.027E-07**	8.968E-05	0.6051	229	**5.427E-05**	**5.760E-05**	-5.79%	NATO	**bottom, out of focus**
7, 1	**0.5080**	**0.1724**	400	266.09	9.0354	**2.027E-07**	1.177E-04	0.3676	143	**4.327E-05**	**5.210E-05**	-16.96%	NATO	**center, on pixel**
7, 2	**0.5080**	**0.1724**	400	266.09	9.0659	**2.027E-07**	1.107E-04	0.3973	155	**4.398E-05**	**5.210E-05**	-15.58%	NATO	**center, on pixel**
7, 3	**0.5080**	**0.1724**	400	266.09	9.0850	**2.027E-07**	8.998E-05	0.5297	206	**4.766E-05**	**5.209E-05**	-8.50%	NATO	**center**
7, 1	**0.5080**	**0.1724**	372	234.58	9.1767	**2.027E-07**	7.798E-05	0.5354	208	**4.175E-05**	**4.568E-05**	-8.61%	NATO	**center**
7, 2	**0.5080**	**0.1724**	373	235.64	9.1710	**2.027E-07**	7.752E-05	0.5046	196	**3.912E-05**	**4.590E-05**	-14.78%	NATO	**center, on pixel**
7, 3	**0.5080**	**0.1724**	373	235.64	9.1605	**2.027E-07**	9.690E-05	0.4187	163	**4.057E-05**	**4.590E-05**	-11.61%	NATO	**center, on pixel**
7, 4	**0.5080**	**0.1724**	373	235.64	9.1637	**2.027E-07**	9.044E-05	0.4974	193	**4.498E-05**	**4.590E-05**	-2.00%	NATO	**center**

Figures 6-9 illustrate IR images of the point target at different locations in the field of view and with slightly different focus settings. The out-of-focus cases correspond to a signal drop by a factor of 2. In Fig. 8, a slight blurring can be seen caused by coma distortion.

Table 1 lists the results for resolved and unresolved targets as measured in the laboratory with the setup described in Fig. 5. Column 3 gives the target diameter in mrad. Each detector element covers an instantaneous field of view of 0.25 mrad. The temperature of the blackbody source behind the target plate is given in column 4. The measured and calculated (real) target intensity contrasts appear in columns 11 and 12, respectively, while the percentage of error is shown in column 13. The yellow shaded lines indicate errors above 10%. Except for a case where the signal was weak, it can be observed that those cases occur mainly for target in-focus, centered on a pixel and in the center of the field of view, which can be explained by the fill-factor effect, as shown in Fig. 4.

Overall, the results are acceptable, considering all the potential sources of error such as the emissivity of the calibration sources and the blackbody source behind the target plate (assumed to be 1.0), the temperature reading of the blackbody, the atmospheric effect in the optical path (assumed negligible, but the spectral response of the camera has a long tail down to 6 μm), the digital noise of the camera, the fill factor effect, which may well sum up to ± 10%. It is seen that the position of the target within the field of view or the focus setting of the camera have little effect on the calculated intensity values as expected, because the broadening of the target image caused by distortions or focus settings distributes the energy over more detector elements, thus compensating for a decrease in the apparent measured radiance values by a larger apparent target area.

7. Conclusion

It has been demonstrated mathematically that one may use an infrared camera that has been radiometrically calibrated in radiance units with extended reference sources, to measure the radiant intensity of point targets. Since no real target is ever, in practice, a point target (because it would need to be infinitesimally small), the notion of a point target is always defined relative to the detector element's projected area at the target range and the projected area of the imager's *PSF*. The intensity of any target is defined as its radiance times its cross-section area. By using an extended-source radiance calibration method to evaluate the intensity of a *point* target, it has been shown that an *apparent* radiance value is effectively determined instead of the real target radiance, as the latter does not completely fill the detector element. To this *apparent* radiance is associated a projected detector element area that is larger than the actual target area, and the exact radiant intensity value is obtained when the two values are multiplied. However, some caution must still be exercised to properly perform the calibration procedure, as described in the calibration methodology detailed in Refs. 1 and 2, to avoid saturation of the reference sources signals, as well as of the target signal during the recording. When a camera with a focal plane array of sensors is used with an

analog recorder, the direct relationship between the true detector elements and the digital pixels, obtained upon digital re-conversion prior to analysis, is lost. In this case, further caution should also be exercised to ascertain that a smooth signal is obtained in the analog video when scanning a point source across the focal plane array. This will prevent the effect of uncorrected dead spaces between detector elements when using the frame grabber re-converted digital pixels for analysis in lieu of the true detector digital signal, by ensuring that the *PSF* is actually larger than a single detector's sensitive area or that spurious dead space effects are eliminated by the electronics bandwidth.

The methodology described in this memorandum has been used successfully by NETE for the analysis of the co-recording measurements taken during the SIRIUS trials in October 2003 and the comparison with the results obtained from the SIRIUS system based on modeling and detector performance parameters has shown a more than satisfactory agreement[1].

[1] D. Dion, Y. Bédard, L. Forand, E. Fortier, P. Chevrette, "DRDC Analysis of the Sirius Warm Weather Trial Data", DRDC Valcartier report to be published.

8. References

1. P. Chevrette, “Calibration of Thermal Imagers”, Proceedings of SPIE on Optical Testing and Metrology, Vol. 661, June 86

2. P. Chevrette, “Calibration Procedure for IR Signature Analysis”, DREV M-2787/86

3. F. Reid, E. Rouleau, “Description of an Infrared Signature Analysis Software, WinISAS”, DRDC Valcartier, TR 2002-117.

Distribution list

Internal distribution

1 - Director General

3 - Document Library

1 - H/DASO

1 - H/SOp

1 - Mr. B. Ricard

1 - Mr. M. Pichette

1 - Mr. V. Larochelle

1 - Dr. D. St-Germain

1 - Mr. J. Dumas

1 - Mr. J. Delisle

1 - Mr. M. Dupuis

1 - Dr. P. Mathieu

1 - Mr. J. Cruickshank

1 - Mr. J. Maheux

1 - Dr. Luc Forand

1 - Mr. D. Dion

1 - Mrs. F. Reid

1 - Dr. D. Vincent

External distribution

1 – DRDKIM (PDF file)

1 - DRDC

1 - SAA

1 - Director Science and Technology (Air)

1 - DSTA 3

1 - Director Science and Technology (Land)

1 - Director Science and Technology (Maritime)

1 - Director Aerospace Equipment Program Management (C) 4-8

1 - DAEPM (C) 4-8-2

1 - DAEPM (C) 4-8-6

1 - DAEPM 5-5-5

1 - Naval Engineering Test Establishment (Eric Fortier)
9401 Wanklyn Street
LaSalle, Québec, H8R 1Z2

1 - NETE (Yves Bédard)

1 - NETE (Rick Masters)

1 - Mr. P. Chevrette (author)
11924 Place Rivard
Québec, Québec, G2A 3N2

DOCUMENT CONTROL DATA

1. ORIGINATOR (name and address)	2. SECURITY CLASSIFICATION (Including special warning terms if applicable)
Defence R&D Canada Valcartier 2459 Pie-XI Blvd. North Val-Bélair, QC G3J 1X8	Unclassified

3. TITLE (Its classification should be indicated by the appropriate abbreviation (S, C, R or U)
Calibrated infrared measurement of point targets using an extended source calibration methodology (U)

4. AUTHORS (Last name, first name, middle initial. If military, show rank, e.g. Doe, Maj. John E.)
Chevrette, P.

5. DATE OF PUBLICATION (month and year)	6a. NO. OF PAGES	6b .NO. OF REFERENCES
January 2005	18	3

7. DESCRIPTIVE NOTES (the category of the document, e.g. technical report, technical note or memorandum. Give the inclusive dates when a specific reporting period is covered.)
Technical memorandum

8. SPONSORING ACTIVITY (name and address)

9a. PROJECT OR GRANT NO. (Please specify whether project or grant)	9b. CONTRACT NO.
11AR19	

10a. ORIGINATOR'S DOCUMENT NUMBER	10b. OTHER DOCUMENT NOS
TM 2004-076	N/A

11. DOCUMENT AVAILABILITY (any limitations on further dissemination of the document, other than those imposed by security classification)

- ☒ Unlimited distribution
- ☐ Restricted to contractors in approved countries (specify)
- ☐ Restricted to Canadian contractors (with need-to-know)
- ☐ Restricted to Government (with need-to-know)
- ☐ Restricted to Defense departments
- ☐ Others

12. DOCUMENT ANNOUNCEMENT (any limitation to the bibliographic announcement of this document. This will normally correspond to the Document Availability (11). However, where further distribution (beyond the audience specified in 11) is possible, a wider announcement audience may be selected.)

13. ABSTRACT (a brief and factual summary of the document. It may also appear elsewhere in the body of the document itself. It is highly desirable that the abstract of classified documents be unclassified. Each paragraph of the abstract shall begin with an indication of the security classification of the information in the paragraph (unless the document itself is unclassified) represented as (S), (C), (R), or (U). It is not necessary to include here abstracts in both official languages unless the text is bilingual).

14. KEYWORDS, DESCRIPTORS or IDENTIFIERS (technically meaningful terms or short phrases that characterize a document and could be helpful in cataloguing the document. They should be selected so that no security classification is required. Identifiers, such as equipment model designation, trade name, military project code name, geographic location may also be included. If possible keywords should be selected from a published thesaurus, e.g. Thesaurus of Engineering and Scientific Terms (TEST) and that thesaurus-identified. If it is not possible to select indexing terms which are Unclassified, the classification of each should be indicated as with the title.)

Defence R&D Canada

Canada's leader in defence
and national security R&D

R & D pour la défense Canada

Chef de file au Canada en R & D
pour la défense et la sécurité nationale

WWW.drdc-rddc.gc.ca